ISSN 0021-3640, JETP Letters, 2017, Vol. 105, No. 3, pp. 158–163. © Pleiades Publishing, Inc., 2017.
Original Russian Text © P.A. Prudkovskii, K.A. Brekhov, K.A. Grishunin, K.A. Kuznetsov, E.D. Mishina, M.S. Fokin, G.Kh. Kitaeva, 2017, published in Pis'ma v Zhurnal Eksperimental'noi i Teoreticheskoi Fiziki, 2017, Vol. 105, No. 3, pp. 142–147.

OPTICS
AND LASER PHYSICS

Photoinduced Gratings in a $Sn_2P_2S_6$ Ferroelectric Crystal with the Period Depending on the Optical Pump Power

P. A. Prudkovskii[a], *, K. A. Brekhov[b], K. A. Grishunin[b], K. A. Kuznetsov[a], E. D. Mishina[b], M. S. Fokin[a], and G. Kh. Kitaeva[a]

[a] *Faculty of Physics, Moscow State University, Moscow, 119991 Russia*
[b] *Moscow Technological University (MIREA), Moscow, 119434 Russia*
* *e-mail: vysogota@gmail.com*

Received July 18, 2016; in final form, December 14, 2016

The light scattering in the form of ring structures in $Sn_2P_2S_6$ crystals at the propagation of intense laser pump radiation along the *b* crystallographic axis is detected. Radiation passing through a crystal is completely scattered into a cone whose angle increases with the pump power and decreases reversibly with a decrease in this power. The observed effect can be attributed to a spontaneous increase in the amplitude of photoinduced bulk diffraction gratings and to the scattering of light on them in the directions where the phase increments of the photorefractive and diffraction natures compensate each other. A similar type of scattering was observed previously in other photorefractive crystals, but the appearance of gratings with the period easily varied by varying the pump power is demonstrated for the first time.

DOI: 10.1134/S0021364017030134

The appearance of radiation that is not due to the addition or subtraction of wave vectors of pump modes at wave mixing in a nonlinear medium is always of interest and usually indicates the development of a certain instability in the medium. Photorefractive media are particularly interesting because the creation of new modes of light is accompanied by the recording of bulk diffraction gratings in the medium. It is well known that the spontaneous growth of noise lattice is possible in photorefractive crystals, which results in the development of so-called photoinduced light scattering, i.e., the scattering of light into a wide cone, which is accompanied by the blooming of the crystal at the place of pump transmission (optical damage) [1–6]. The ends of wave vectors of noise gratings lie on a certain sphere; i.e., their set is two-dimensional. Gratings with low wave vectors, which are almost perpendicular to the wave vector of the pump beam, usually have the largest amplitude. In the case of four-wave synchronism, the one-dimensional subset of lattices can be enhanced and scattering on them is manifested in the form of a narrow cone with an apex angle determined by the synchronism condition. This effect was referred to as parametric holographic scattering [7–9].

Less well known is a more nontrivial effect: in the field of two counterpropagating pump beams, the enhancement of gratings whose wave vector is almost parallel to the wave vector of the pump can occur. This phenomenon was detected in media with Kerr nonlinearity [10], in niobate lithium photorefractive crystals [11, 12], and in $KNbO_3$ [13, 14] and $BaTiO_3$ [15] crystals. This instability results in the growth of a one-dimensional set of bulk gratings corresponding to scattering of light in the form of a narrow cone at an angle at which the phase increments of the diffraction and nonlinear natures compensate each other [16]. The enhancement of three gratings whose transverse components of wave vectors form a regular triangle can sometimes occur manifesting itself in the scattering as point hexagonal structures [13–15, 17]. A conic instability can also be observed in schemes with a single pump beam [11–14] if the opposite beam appears because of the reflection of incident radiation from the back face of the crystal and is enhanced owing to energy exchange with the direct pump beam [18]. The effect in any case is threshold in the pump intensity, but the analytical solution for the threshold of instability [16, 17] can be obtained only for identical intensities of pump beams or for ideal reflection from the back face of the crystal and does not describe the general case with an arbitrary relation between the intensities of counterpropagating beams.

This work presents the observation of conical instability in the scheme with one pump beam in an additional crystal with photorefractive properties, in $Sn_2P_2S_6$ (SPS). The detected scattering has a feature that has not yet been observed: the apex angle of the scattering cone significantly depends on the pump intensity and can be varied by simple variation of the power of incident radiation. The second characteristic

feature of the observed effect is the possibility of the complete transfer of the energy of radiation incident on the crystal to scattering cones.

The SPS crystal has very interesting physical properties, in particular, a quite efficient and relatively fast photorefractive response: the time of creation of stationary photorefractive gratings in a number of experiments was about several milliseconds [19]. This crystal at room temperature is a ferroelectric semiconductor (the width of the band gap is 2.35 eV [20]), but it transforms into a paraelectric phase at a small heating to ~64°C [21]. The repolarization of domains requires a quite low coercive field of ~750 V/cm [22]. The optical, nonlinear optical, crystallographic, electronic, and photorefractive properties of this crystal, as well as phonon and polaron resonances and defects in it, are actively studied [23–29].

EXPERIMENT

Figure 1a shows the layout of the experiment including a titanium–sapphire laser with the pump wavelength varying in the range of 700–1000 nm, a pulse repetition frequency of 80 MHz, and the duration of pulses of ~100 fs. The direction of the linear polarization of pump was varied by means of a half-wave plate. Laser radiation was focused on the crystal with a thickness of about 0.5 mm by means of a lens with a focal length of 10 cm. Radiation transmitted through the crystal was incident on a screen located at a distance of 25 cm from the sample and its image was detected on a camera. In order to observe the spatial structure of reflected radiation, a semitransparent glass plate placed in front of the crystal deflected a fraction of reflected radiation to the second screen located laterally. To select radiation transmitted through the crystal in the polarization, we used a Glan prism. The input and output faces of the crystal were perpendicular to the b axis of the unit cell of the crystal, which has a monoclinic point group of symmetry m at room temperature. Figure 1b shows the crystallographic axes of the SPS crystal: the mutually orthogonal X and Z axes lie in the plane of the input and output faces, and the Y axis is perpendicular to the input face. It is known that the SPS crystal is optically biaxial. One of the axes of the indicatrix of refractive indices coincides with the Y axis, and the X' and Z' axes lie in the $\langle 010 \rangle$ plane and are turned with respect to the Z and X crystallographic axes by a certain angle (α in Fig. 1b), which depends on the temperature and wavelength of radiation. According to [30], at room temperature and in the range of pump wavelength of 700–1000 nm appropriate for our measurements, the angle α varies in a narrow range of 44°–48°.

When the average power and peak intensity of the incident laser radiation were below 60 mW and $I_p = 180$ MW/cm^2, respectively, we did not observe any significant distortions of the spatial structure of

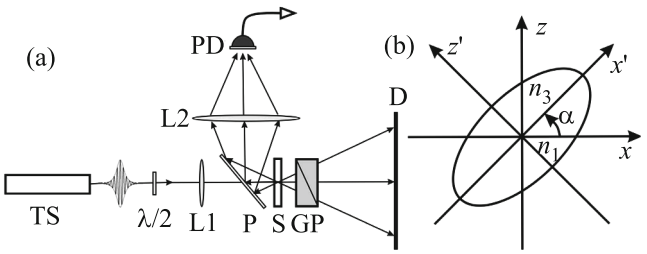

Fig. 1. (a) Layout of the experimental setup: (TS) titanium–sapphire laser, (L) lenses, (GP) Glan prism, (D) screen, (PD) photodetector, (P) glass plate, and (S) SPS crystal. (b) Crystallographic axes of the SPS crystal (the Y axis is perpendicular to the plane of the figure) and the ellipse of refractive indices in the XZ plane.

the transmitted and reflected beams. However, at a further increase in the pump power, rings appeared on both screens fixing the structure of the transmitted and reflected radiation, and the spot of the direct passage of the pump beam on the screen behind the crystal gradually disappeared. It is noteworthy that the appearance of a ring structure, i.e., the development of conical instability, was observed at the incidence of the pump beam on the crystal plate only from one of two possible sides: when the sample was turned by 180°, no ring scattering was observed. This property is explained by the necessity of the counterpropagating light beam for the development of instability: the direction of energy exchange between the pump beam and the counterpropagating light beam changes the sign when the crystal is turned [18]. As a result, the light beam reflected from the back face of the crystal is enhanced at one orientation of the crystal and is weakened at the opposite orientation.

Figure 2 shows the images of laser radiation with a wavelength of 700 nm and an average power of 110 mW transmitted through the crystal. The images in Figs. 2a–2c correspond to the polarization of the incident radiation along the Z crystallographic axis of the crystal, whereas Figs. 2d–2f correspond to the case where the polarization of the pump beam with the same power is almost parallel to one of two mutually perpendicular axes of the indicatrix of the crystal. It is seen that images of the transmitted radiation consist of two concentric rings whose polarizations are mutually orthogonal and correspond to the principal directions of the optical indicatrix: the inner and outer rings in all photographs are polarized along the X' and Z' axes, respectively. When the pump power remains constant, the direction of its polarization affects only the ratio of the intensities of the two rings. Using the data from [30] on the dispersion of the principal refractive indices of the crystal, it is easy to show that the splitting of rings with mutually orthogonal polarizations beyond the crystal is due to the refraction of waves on the output surface, whereas a ring inside the crystal is single.

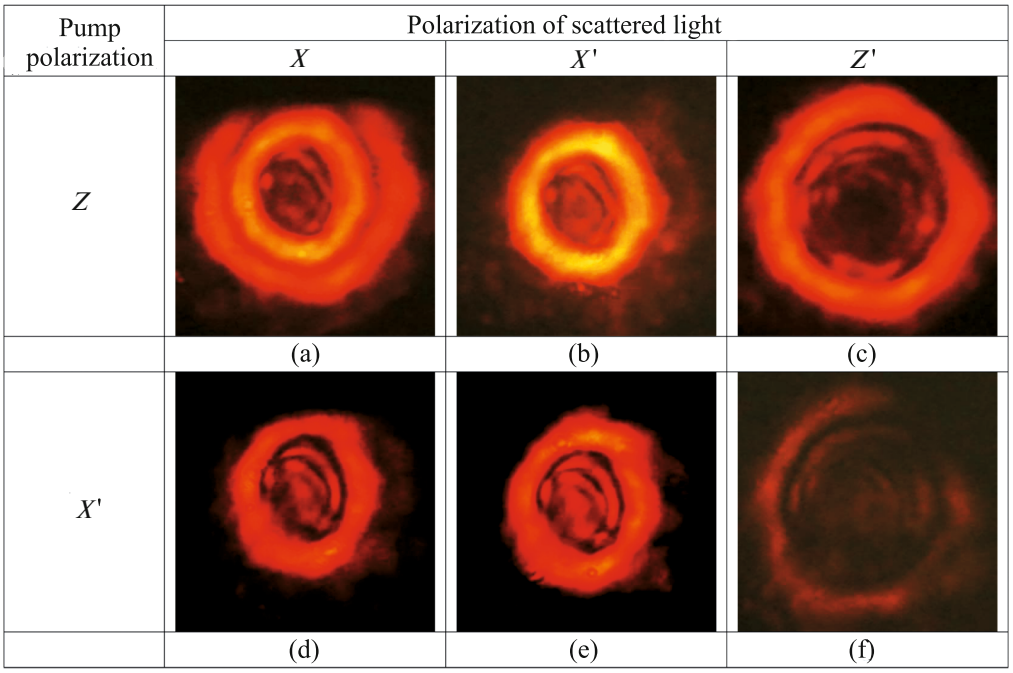

Fig. 2. (Color online) Images of scattered radiation appearing at a power of 110 mW and a wavelength of 700 nm of pump radiation polarized along the (a–c) Z crystallographic axis and (d–f) X' axis of the optical indicatrix. Transmitted radiation is polarized along the (a, d) X crystallographic axis, (b, e) X' axis of the optical indicatrix, and (c, f) Z' axis of the optical indicatrix.

The most interesting feature of the observed ring structure is the direct relation of the apex angle of the scattering cone θ with the power of the incident radiation (Fig. 3). The radius of the rings observed in the transmitted and reflected light increases monotonically with the power rise from the threshold intensity and up to quite high powers. The relaxation time of a new scattering picture after a change in the pump power varied in the range of 0.1–1 s. Figure 4 shows the experimental dependences of the apex angle of the cone scattering θ on the intensity of the radiation incident on the crystal measured for various pump wavelengths. Each of the dependences contains a segment in which the scattering angle increases with the pump intensity, and the slope of a dependence is larger for a smaller pump wavelength. However, an increase in the scattering angle ceases at sufficiently large angles and the transition to this regime is seen in Fig. 4 for the sharpest dependence corresponding to a pump wavelength of 700 nm. The picture of establishing the steady distribution of the power of transmitted radiation in this segment is different: the radius of the ring increases at times less than or about 0.4 s and, then, decreases sharply in a time smaller than 0.1 s. Continuous pulsations of radii of rings with a period of about several tenths of a second were observed in this stage in longer samples with a thickness of ~3 mm at certain powers. The authors of [11] treated a similar nonstationary behavior of conical scattering of light as a transition to an autowave mode. Indeed, a large response time of photorefraction can be responsible for autowave processes, which significantly change the dynamics of scattering [31]. However, another reason for such a nonstationary behavior of the rings could be the heating of the crystal at high pump powers, which means an approach to the phase transition point. A further increase in the pump power led to the decay of rings into small-scale structures and the appearance of a smeared spatially inhomogeneous spot instead of rings on the screen (see Fig. 3d). Finally, at powers equal to and higher than 175 mW (for the pump beam with a wavelength of 700 nm), a complex picture of scattering disappeared and transmitted radiation formed a spot with the diameter of the incident pump beam.

DISCUSSION OF THE RESULTS

The observed scattering in the form of ring structures in SPS crystals is similar to scattering previously observed in other photorefractive crystals [11–15], but has two important differences. First, the intensity of ring scattering in all previous works was a small fraction of the pump intensity, whereas the pump beam in our case disappears completely at the output of the crystal, i.e., the pump is completely transferred to scattering rings. Second, the radius of rings in our case (i.e., the transverse component of the wave vector $q_\perp$ of bulk gratings written in the crystal) depends on the pump intensity, whereas the radius of stationary scattering rings in all previous works did not change.

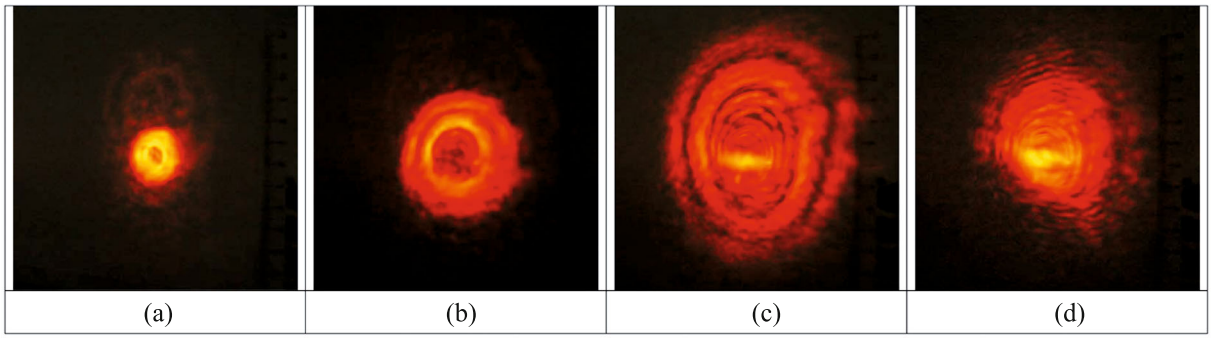

Fig. 3. (Color online) Ring structures in scattered light at a pump power of (a) 89, (b) 113, (c) 129, and (d) 150 mW.

As was mentioned above, in the case of identical intensities of counterpropagating beams, an analytical expression can be obtained for the threshold of conical instability [16, 17]. The intensity reflection coefficient from the back face of the SPS crystal is approximately 25%. Consequently, the opposite pump beam is certainly weaker than the direct pump beam. In the case of an arbitrary relation between the intensities of pump beams, the threshold of instability can be obtained by numerically solving equations similar to those obtained in [16]. We note that we performed a linear analysis of the interaction of weak modes of scattered light in the field of strong inexhaustible counterpropagating pump beams. Figure 5 shows the rate of growth of conical instability thus obtained in the coordinates $(q_\perp, \eta L I_p)$, where I_p is the pump intensity, L is the length of the crystal, and the parameter η describes the efficiency of energy exchange between optical modes in the crystal because of photorefraction. It is seen that the region of instability with the smallest component $q_\perp$ appears first and the rate of growth in it remains the highest at a further increase in the intensity. For this reason, it is not surprising that ring structures corresponding to the unchanged minimally possible transverse component of the wave vector were observed in [11–15]. However, if the pump power is almost completely transferred to ring structures, as in our case, ring structures with the minimum component $q_\perp$ can serve as secondary pump structures for scattering with large angles. An increase in the radius of rings with an increase in the pump intensity is likely due to the nonlinear interaction of modes with various transverse components of the wave vector. Unfortunately, the nonlinear analysis of the interaction of scattering modes corresponding to different regions of instability in Fig. 5 with allowance for exhaustion of pump is too complicated and is beyond the scope of this work.

The so-called local and nonlocal photorefractive responses of the crystal are usually distinguished. The local response leads to the formation of bulk gratings, which are not displaced with respect to the interference pattern of radiation and produce only the phase

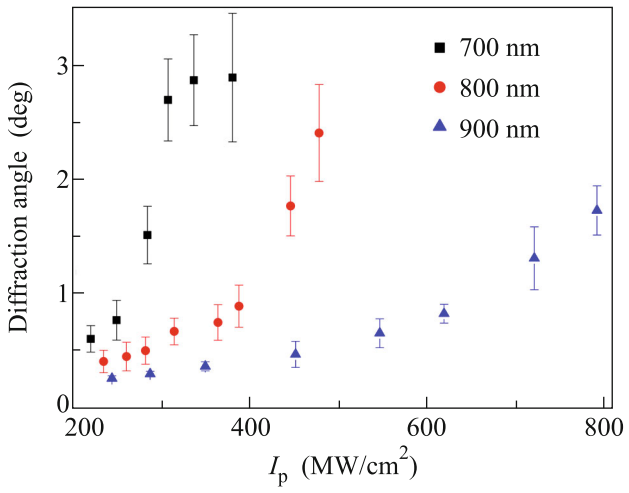

Fig. 4. (Color online) Diffraction angle versus the pump intensity with various wavelengths.

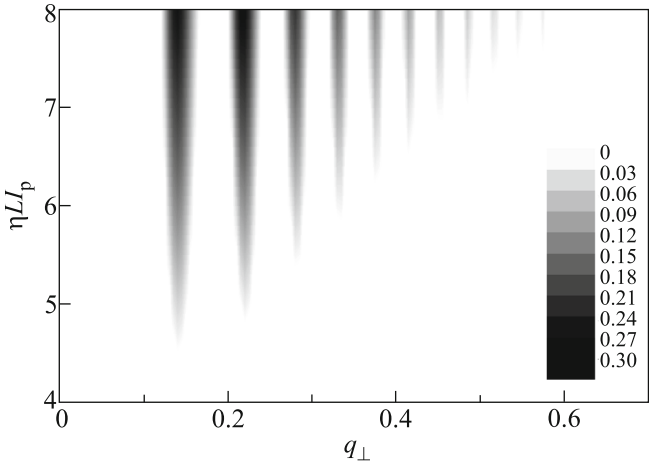

Fig. 5. Threshold of conical instability and the growth rate of gratings with the transverse wave vector $q_\perp$ according to the numerical integration in $(q_\perp, \eta L I_p)$ coordinates (in arbitrary units).

increment in scattered light. The nonlocal response corresponds to gratings shifted by half the wavelength with respect to the interference pattern and leads to the energy exchange between radiation modes. Figure 5 is plotted for approximately equal local and nonlocal responses of the crystal; in this case, the threshold of conical instability is $\eta L I_p \approx 4.5$. However, it is known that the diffusion mechanism of photorefraction, which is responsible for the nonlocal response, prevails in SPS crystals. The local response in these crystals, which is associated with the photogalvanic effect, is several orders of magnitude weaker [32]. The numerical analysis shows that the threshold of instability in this case will be several orders of magnitude higher; i.e., it should be expected at a level of 10^3–10^5.

The quantity $\eta L I_p$ for our experimental conditions can be estimated as follows. The parameter η characterizing the photorefractive response of a diffusion nature can be represented in the form $\eta = renD/(\lambda^2 \sigma I_s)$ [33], where r is the component of the electro-optical tensor; λ is the pump wavelength; n and D are the concentration and coefficient of diffusion of charge carriers, respectively; σ is the conductivity of the crystal; and I_s is the parameter describing the saturation effects at the photoexcitation of charge carriers. Since $D \sim kT\mu/e$ and $\sigma \sim en\mu$, where μ is the mobility of charge carriers, we obtain $\eta L I_p \sim (rkT/(\lambda e))(L/\lambda)(I_p/I_s)$. The electro-optical coefficient in SPS crystals is on the order of $r \sim$ 100 pm/V and the parameter of saturation is estimated as $I_s \sim 7$ W/cm^2 [34]. Therefore, for our experimental conditions at the threshold intensity $I_p = 180$ MW/cm^2, we obtain $\eta L I_p \sim 3 \times 10^4$ in qualitative agreement with our theoretical estimates.

The electrostatic field of separated charges can be estimated similarly as $\mathscr{E} \sim (kT/(\lambda e))(I_p/I_s) \approx 5 \times 10^9$ V/cm. It is seen that this field is several orders of magnitude higher than the coercive field in SPS crystals. This means that the detected conical instability in SPS crystals, which results in the recording of bulk diffraction gratings with a transverse component of the wave vector depending on the pump intensity, should be accompanied by processes of repolarization of the crystal and the formation of structures of ferroelectric domains. The study of formed domain structures and the possibility of their rearrangement by the simple variation of the optical pump power can be a very interesting continuation of this work.

We are grateful to Yu.M. Vysochanskii for the samples provided at our disposal, to A.M. Buryakov and V.R. Bilyk for assistance in the experiment, and to A.A. Ezhov for useful consultations. This work was supported by the Ministry of Education of Science of the Russian Federation (project no. 14.Z50.31.0034) and by the Russian Foundation for Basic Research (project nos. 14-22-02091 and 16-02-00258 and state contract no. 3.7500.2017/P220).

REFERENCES

1. W. Phillips, J. J. Amodei, and D. L. Staebler, RCA Rev. **33**, 94 (1972).
2. I. F. Kanaev, V. K. Malinovsky, and V. I. Sturman, Opt. Commun. **34**, 95 (1980).
3. V. V. Voronov, I. R. Dorosh, Yu. S. Kuz'minov, and N. V. Tkachenko, Sov. J. Quantum Electron. **10**, 1346 (1980).
4. P. A. Augustov, M. Reinfelde, and K. K. Shvarts, Appl. Phys. A **29**, 169 (1982).
5. E. M. Avakyan, K. T. Belabaev, and S. G. Odulov, Sov. Phys. Solid State **25**, 1887 (1983).
6. F. Guibaly and L. Yong, Ferroelectrics **46**, 201 (1983).
7. S. Odoulov, K. Belabaev, and I. Kiseleva, Opt. Lett. **10**, 31 (1985).
8. I. N. Kiseleva, V. V. Obukhovskii, and S. G. Odulov, Sov. Phys. Solid State **28**, 1673 (1986).
9. D. A. Temple and C. Warde, J. Opt. Soc. Am. B **3**, 337 (1986).
10. J. Pender and L. Hesselink, J. Opt. Soc. Am. B **7**, 1361 (1990).
11. V. V. Obukhovskii and A. V. Stoyanov, Sov. J. Quantum Electron. **15**, 367 (1985).
12. S.-M. Liu, G.-Y. Zhang, J.-L. Wang, X.-Y. Ma, and Y.-F. Fu, Opt. Commun. **70**, 185 (1989).
13. T. Honda, Opt. Lett. **18**, 598 (1993).
14. N. V. Kukhtarev, T. V. Kukhtareva, H. J. Caulfield, P. P. Banerjee, H.-L. Yu, and L. Hesselink, Opt. Eng. **34**, 2261 (1995).
15. T. Honda and H. Matsumoto, Opt. Lett. **20**, 1755 (1995).
16. B. I. Sturman and A. I. Chernykh, J. Exp. Theor. Phys. **84**, 881 (1997).
17. P. M. Lushnikov, J. Exp. Theor. Phys. **86**, 614 (1998).
18. I. F. Kanaev, V. K. Malinovskii, and B. I. Sturman, Sov. Phys. JETP **47**, 834 (1978).
19. S. G. Odoulov, A. N. Shumelyuk, U. Hellwig, R. A. Rupp, A. A. Grabar, and I. M. Stoyka, J. Opt. Soc. Am. B **13**, 2352 (1996).
20. R. V. Gamernyk, Yu. P. Gnatenko, P. M. Bukivsij, P. A. Skubenko, and V. Yu. Slivka, J. Phys.: Condens. Matter. **18**, 5323 (2006).
21. R. M. Yevych and Yu. M. Vysochanskii, Condens. Matter Phys. **11**, 417 (2008).
22. C. D. Carpentier and R. Nitsche, Mater. Res. Bull. **9**, 1097 (1974).
23. M. I. Gurzan, A. P. Buturlakin, V. S. Gerasimenko, N. F. Korde, and V. Y. Slivka, Sov. Phys. Solid State **19**, 1794 (1977).
24. A. Anema, A. Grabar, and T. Rasing, Ferroelectrics **183**, 181 (1996).
25. A. A. Grabar, I. V. Kedyk, M. I. Gurzan, I. M. Stoika, A. A. Molnar, and Y. M. Vysochanskii, Opt. Commun. **188**, 187 (2001).

26. D. Haertle, G. Caimi, A. Haldi, G. Montemezzani, P. Gunter, A. A. Grabar, I. M. Stoika, and Y. M. Vysochanskii, Opt. Commun. **215**, 333 (2003).
27. M. Imlau, V. Dieckmann, H. Badorreck, and A. Shumelyuk, Opt. Mater. Express **1**, 953 (2011).
28. Yu. Vysochanskii, K. Glukhov, K. Fedyo, and R. Yevych, Ferroelectrics **414**, 30 (2011).
29. K. A. Grishunin, K. A. Brekhov, and O. V. Samotokhin, Ross. Tekhnol. Zh. **2** (7), 134 (2015).
30. D. Haertle, A. Guarino, J. Hajfler, G. Montemezzani, and P. Günter, Opt. Express **13**, 2047 (2005).
31. P. A. Prudkovskii, Quantum Electron. **41**, 30 (2011).
32. Y. W. Cho, S. K. Choi, and Yu. M. Vysochanskii, J. Mater. Res. **16**, 3317 (2001).
33. V. V. Obukhovskii and A. V. Stoyanov, Sov. J. Quantum Electron. **15**, 367 (1985).
34. A. A. Grabar, M. Jazbinsek, A. N. Shumelyuk, Y. M. Vysochanskii, G. Montemezzani, and P. Gunter, Springer Ser. Opt. Sci. **114**, 640 (2007).

Translated by R. Tyapaev